Pergamon

Bioorganic & Medicinal Chemistry, Vol. 4, No. 6, pp 803–813, 1996

0968-0896/96 $15.00+0.00

S0968-0896(96)00070-3

A Microgonotropen Pentaaza Pentabutylamine and its Interactions with DNA

Dipanjan Sengupta, Andrei Blaskó and Thomas C. Bruice*
Department of Chemistry, University of California, Santa Barbara, CA 93106, U.S.A.

Abstract—The central pyrrole of a site-selective DNA minor groove binding tripyrrole peptide (**1**) has been attached to N-protected pentaazapentacosanoic acid (**17**) via a $-(CH_2)_3-NHCO-(CH_2)_3-$ linker to provide **19**, subsequent deprotection provided the pentaaza microgonotropen **4**. The polyamine moiety of **4** reaches out of the minor groove and binds to the phosphate backbone of DNA. We find when employing Hoechst 33258 (Ht) as a fluorescent titrant to follow binding of **4** to the hexadecameric duplex d(GGCGCAAATTTGGCGG)/(CCGCCAAATTTGCGCC) and by ^{1}H NMR titration of d(CGCAAATTTGCG)$_2$ with **4** that the latter forms both 1:1 and 2:1 dsDNA complexes. Certain aspects of the structure of **4**:d(CGCAAATTTGCG)$_2$ complex derived via ^{1}H NMR are discussed. The electrophoretic mobilities of ϕX-174 DNA digested with *Hae*III endonuclease restriction fragments complexed to **4** shows that the latter brings about a greater conformational change in the DNA fragments than observed previously with other microgonotropens. Copyright © 1996 Elsevier Science Ltd

Introduction

There has been considerable interest in reagents capable of sequence selective nonintercalative complexation to DNA. Small organic compounds able to complex to the minor groove of B-DNA[1] have drawn much interest in recent years. A crescent shape to match the natural curvature of the minor groove of B-DNA is a common motif of each of these molecules.[2] New among the minor groove binding molecules are the microgonotropens[3] **5**, **6** and **1** (Chart 1). Based upon distamycin, the characteristic shape of microgonotropens is dictated by the peptide linkages between three 1-methyl-4-aminopyrrole-2-carboxylic acid residues.[2a] Our microgonotropen design is based on the concept of two essential parts: (i) a recognition unit (the selective DNA minor groove binding molecule)[1] that serves as a carrier and (ii) a polyamine moiety reaching out of the minor groove and capable of firmly binding to the phosphodiester backbone. The objective of the microgonotropen design is to occupy a sequence determined portion of both the minor and major grooves. Tight binding is desired in order that the microgonotropen is useful as a drug. It is important to know what structural features most favors strong polyamine complex formation. Is it best to have the protonated amino functions bunched as with a tren side chain or is tighter binding seen with a simple single chain polyamine?

In a previous synthesis[4] microgonotropen **1** was prepared with a $-(CH_2)_3NH_2$ linker arm on the central pyrrole nitrogen. Various agents potentially capable of interacting with the major groove can be conveniently covalently attached to the tripyrrole carrier through a coupling reaction with the amino function of the linker arm of **1**. Thus, compound **1** was designed to be a 'truck' to carry funtionalities to the DNA major groove. We report here the synthesis of microgonotropen **4**, which has a pentaaza pentabutylamine moiety attached to the central pyrrole nitrogen. In addition, the association of **4** to DNA has been evaluated by fluorescence and NMR techniques. The electrophoretic mobility of DNA fragments complexed by **4** has been determined as a means to access the ability of **4** to change the DNA conformation.

The procedure, as used for the preparation of **4**, is a simplifying improvement over the synthetic procedures used for the dien- and tren-microgonotropens (**5a–c** and **6a,b** in Chart 1). Our purpose is to generate a series of polyamine microgonotropens in order to ascertain what structural features lead to best binding to DNA and best behavior as agents to prevent transcription factor binding.

Results

Synthesis

A convergent synthetic strategy was envisioned in which **4** was synthesized by reacting microgonotropen **1** with *N*-protected pentaazapentacosanoic acid (**17**). The synthesis of polyamine **17** was based on an S_N2 substitution reaction of an appropriate tosylate with 4-amino-1-butanol (**7**) (Scheme 1). 4-Carbobenzyloxyamino-1-butanol (**8**) was converted to tosylate **9**, which was condensed with 4-amino-1-butanol in DMF at 80 °C to yield the dimer **10** in 63% yield. The amino nitrogen in the dimer **10** was protected with a *tert*-butoxycarbonyl (Boc) group and tosylated to give compound **11** in 66% yield. Repeating the same

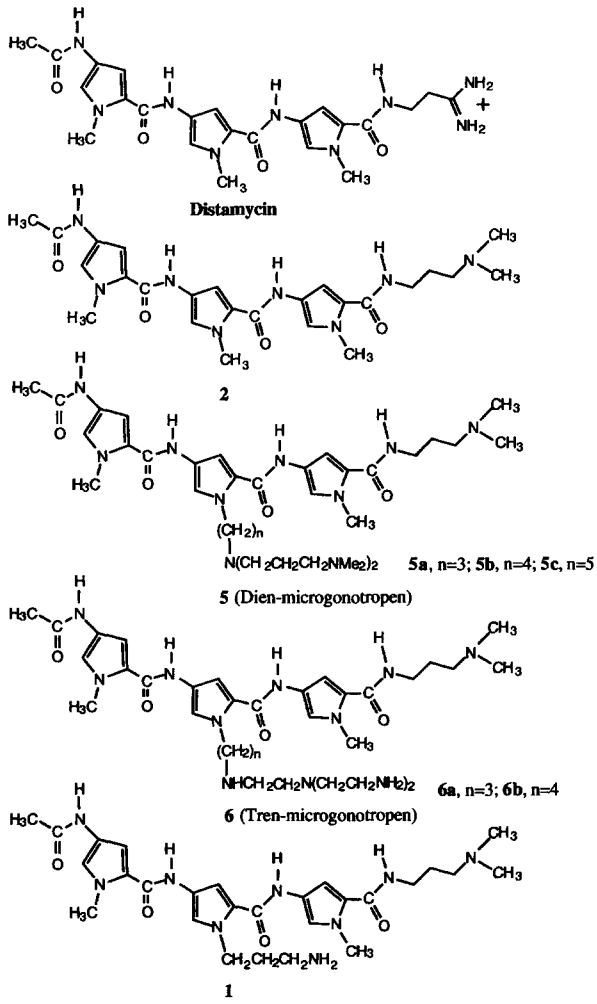

Chart 1.

sequence of reactions (Scheme 1) ultimately provided **16**.

After protecting the amino nitrogen of **16** as N-Boc, the terminal hydroxyl was oxidized to a carboxylic acid by treating with PDC in DMF[5] at room temperature to give **17** (40% yield). The acid **17** was reacted[6] with **1** in the presence of DCC and HOBT in DMF at room temperature (Scheme 2) to give **19** in 55% yield. The carbobenzyloxy protecting group in **19** was removed by catalytic hydrogenation (10% Pd–C) and the Boc protecting groups were removed by protonolysis using 40% TFA in CH_2Cl_2 (Scheme 2). Finally, **4** was generated from its TFA salt by treatment with Dowex 1×8–100 ion exchange resin (OH^- form) in methanol. Compound **16** was converted to **18** (95% yield) using the same reactions as has been used to convert **19** to **4**.

The ^1H signals of **4** were assigned from the DQF-COSY experiment (Table 1). In DMSO-d_6 the polyamino substituent's methylene protons are heavily overlapped at 1.4 and 2.4 ppm. There are cross peaks between R3(NH) and R3(1) and R2(NH) and R2(3) (**4** in Scheme 2). The assignments of all other signals are consistent with the earlier assignments of the microgonotropens.[7]

Equilibrium constants for the association of 4 with d(GGCGCAAATTTGGCGG)/ d(CCGCCAAATTTGCGCC)

The equilibrium association constants were determined in aqueous solutions at 35 °C (2.8 mL solutions containing 0.01 M phosphate buffer, pH 7.0 and 0.01 M KCl). The concentration of **4** was confirmed by peak integration of ^1H NMR resonances, with resonances of an approximately equivalent but known concentration

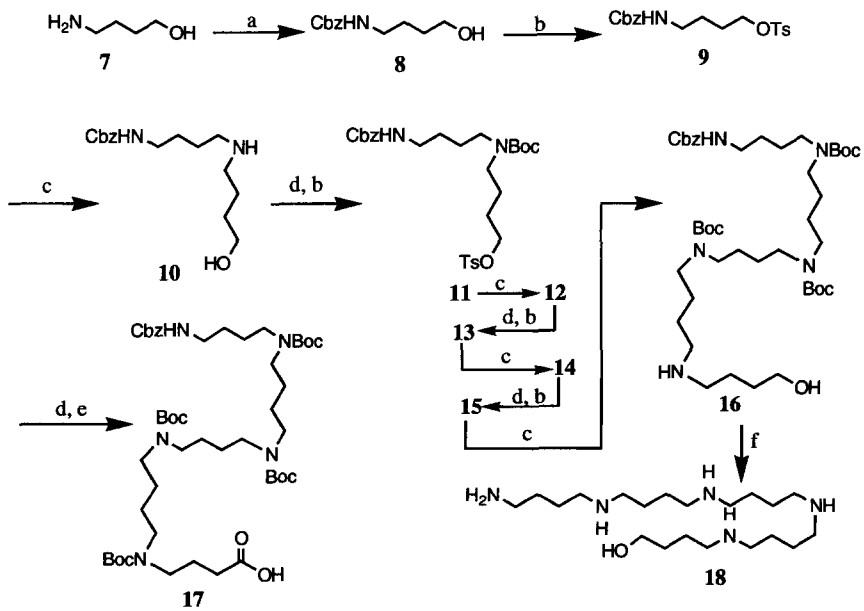

Scheme 1. Reagents and conditions: (a) benzyl chloroformate, aq Na_2CO_3, rt, overnight; (b) tosyl chloride, pyridine, 0–5 °C, 3 h; (c) **7**, DMF, 80–85 °C; (d) *tert*-butyl-dicarbonate, CH_2Cl_2, 0–5 °C, 25 min; (e) PDC, DMF, rt, 4 h; (f) H_2 Pd–C, 40% TFA–CH_2Cl_2, Dowex ion exchange resin (OH^-) form.

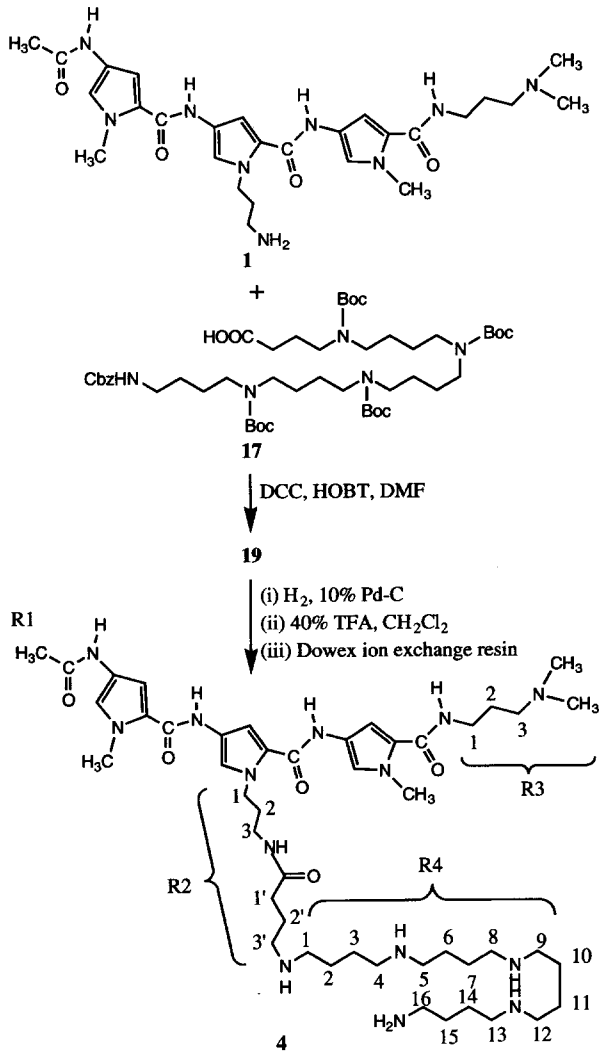

Scheme 2.

Table 1. ^{1}H chemical shifts of **4** in DMSO-d_6 at 25 °C[a]

		R1	R2	R3	R4	R5[e]	R6[e]
CH_3		1.97		2.14		3.80	3.83
CH_2	(1)		4.31	3.09	2.50		
	(2)		1.81	1.62	1.41		
	(3)		3.01	2.25	1.37[b]		
	(4)				2.44[c]		
	(1′)		2.03				
	(2′)		1.68; 1.44[d]				
	(3′)		2.98				
	(14), (15)				1.60		
	(16)				2.09		
NH			7.83	8.07		9.90	9.92
NH	(1–4)				5.30		

[a]In ppm relative to TMS.
[b]The same value for CH_2 (**3**, **6**, **7**, **10** and **11**).
[c]The same value for CH_2 (**4**, **5**, **8**, **9**, **12** and **13**).
[d]Nonequivalent resonances.
[e]R5 and R6 = pyrrole N-CH_3's of R1 and R3.

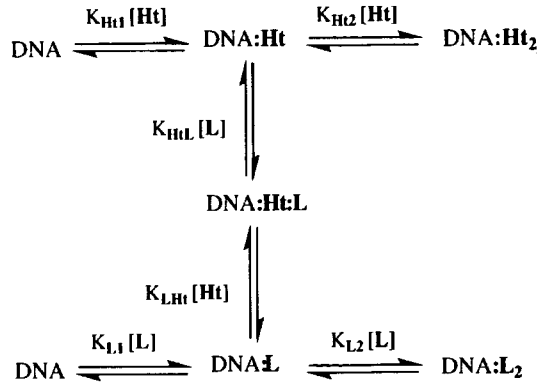

Scheme 3.

of 2,4,6-trimethyl benzoate. The extent of complex formation was determined by titration of a solution of d(GGCGCA$_3$T$_3$GGCGG)/d(CCGCCA$_3$T$_3$GCGCC) containing a known concentration of **4** with Hoechst 33258. Increase in fluorescence is due to formation of dsDNA:**Ht**, dsDNA:**Ht2** and dsDNA:**Ht:L** (**4** is indicated as **L**) complexes[8] as **Ht** competes with **4** for a common A_3T_3 minor groove binding site.

Equation (1), derived from Scheme 3, relates the fluorescence (F) to

$$F=\frac{\Sigma\Phi K_{Ht1}[\mathbf{Ht}]\ (0.5+K_{Ht2}[\mathbf{Ht}]+0.5\ K_{HtL}\ [\mathbf{L}]\ Q')}{1+K_{Ht1}[\mathbf{Ht}]+K_{Ht1}K_{Ht2}[\mathbf{Ht}]^2+K_{Ht1}K_{HtL}[\mathbf{Ht}][\mathbf{L}]+K_{L1}[\mathbf{L}]+K_{L1}K_{L2}[\mathbf{L}]^2} \quad (1)$$

each of the equilibrium binding constants, the total fluorescence (ΣF), the total [**L**] and the total [**Ht**]. The rationale behind the derivation of equation (1) has been described in considerable detail.[9] The values of $K_{Ht1}=3.75\times10^7\ M^{-1}$ and $K_{Ht2}=1.45\times10^9\ M^{-1}$ used in this study were determined and reported previously.[9] The equilibrium association constants calculated as best fits to the experimental data points when **L** represents **4** as in equation (1) are presented in Table 2. Q' represents the internal quenching constant by **4** of fluorescence of Ht in the complex DNA:**Ht**:**4**. The best value of Q' determined is 0.5. Plots of fluorescence (F) versus [**Ht**] with **4** at 5.0×10^{-9}, 7.5×10^{-9}, and 1.0×10^{-8} M and d(GGCGCA$_3$T$_3$GGCGG)/d(CCGCCA$_3$T$_3$GCGCC) at 5.0×10^{-9} are shown in Figure 1.

^{1}H NMR titration of d(CGCAAATTTGCG)$_2$ with 4

The ^{1}H NMR signals of the three A•T and the three G•C imino protons (in H_2O:D_2O 9:1) are at 13.5–14.0 and 12.5–13.2 ppm, respectively.[11] The A•T imino signals at 13.62, 13.72 and 13.89 ppm are sharp, whereas the G•C imino signals exhibit two well defined resonances at 13.07 and 12.68 ppm and one (the terminal G•C base pairs) very broad resonance as a shoulder of the signal at 13.07 ppm, centered at ca. 12.9 ppm (Fig. 2). This broad signal is a result of the fraying of the end base pairs.[12] It was shown that by lowering the temperature, the broad G•C signals of the dsDNA and its complexes sharpen.[11] The titration

Table 2. A comparison of the mean logarithmic values of the equilibrium association constants for **1**, **2**, **4**, **6a**, **6b** and distamycin to the hexadecameric duplex d(GGCGCA$_3$T$_3$GGCGG)/d(CCGCCA$_3$-T$_3$GCGCC)

Ligand	log K_{L1}	log K_{L2}	log $K_{L1}K_{L2}$	log K_{HtL}
2[a,b]	6.8	6.2	13.0	−1.2
4[c,d]	8.6	8.8	17.4	10.7
1[c,e]	8.4	8.0	16.4	9.5
6[a,b]	9.2	9.2	18.4	10.7
6b[a,b]	8.9	9.0	17.9	10.3
Distamycin[a,b]	7.6	8.4	16.0	8.8

[a]Reactions were performed in H_2O, 0.01 M phosphate buffer, pH 7.0 and 0.01 M NaCl at 35 °C.
[b]Ref. 3d.
[c]Reactions were performed in H_2O, 0.01 M phosphate buffer, pH 7.0 and 0.01 M KCl at 35 °C.
[d]Mean values and standard deviations (sn) are the result of experiments at 3.0×10^{-9}, 5.0×10^{-9}, 6.0×10^{-9}, 7.5×10^{-9}, 9.0×10^{-9} and 1.0×10^{-8} M in **4**.

was carried out in 0.25 mol equiv steps up to 1:1 **4**/dsDNA and 0.50 mol equiv steps from 1:1 to 2.5:1 **4**/dsDNA. At 0.25:1 **4**/dsDNA new resonances appear in the A•T (13.48 and 13.98 ppm) and the G•C (12.60 and 12.79 ppm) regions. There is a slight broadening of the imino resonances ($\nu_{1/2}$ 15–30 Hz) when increasing from 0 to 1 mol equiv of **4**/dsDNA. The broadening increases to 60–150 Hz when reaching the 2:1 composition of **4**/dsDNA. The A•T region experiences greater broadening than the G•C region. We saw two sets of nonequivalent resonances at 2:1 **4**/dsDNA. While the G•C signal at 13.07 remained unchanged up to 1:1 **4**/dsDNA, at 2:1 **4**/dsDNA this changed to 14.00 ppm and the broad signal at 12.9 ppm sharpens. At 2:1 **4**/dsDNA there was some precipitation.

The titration of d(CGCAAATTTGCG)$_2$ with **4** was also followed in D_2O at the dsDNA concentration of 4×10^{-4} M. The thymidine CH_3 signals resonate in the 1.2–1.8 ppm region. By titration of dsDNA with **4** these signals change and become two nonequivalent sets at 1:1 and also at 2:1 mol ratios of **4**/dsDNA. The titration was also followed in the aromatic 7.0–8.5 ppm region. There was line broadening as the titration progressed, especially in the case of the minor groove pointers (e.g., H1′ and H6/8). We did not see any further changes above 2:1 mol ratio of **4**/dsDNA.

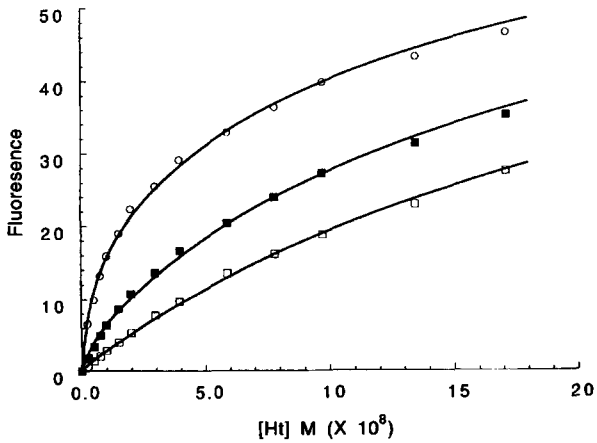

Figure 1. Representative plots of fluorescence (F, in arbitrary units) versus total Hoechst 33258 (**Ht**) concentration at pH 7.0 and 35 °C for **4** at 5.0×10^{-9} M (○), 7.5×10^{-9} M (■) and 1.0×10^{-8} M (□) in the presence of 5.0×10^{-9} M d(GGCGCA$_3$T$_3$GGCGG)/d(CCGCCA$_3$T$_3$GCGCC). The theoretical curves which fit the points were computer generated by optimizing the constants in equation (1).

Electrophoretic mobility shift assay

The effect of **4** binding to ϕX-174 DNA digested with *Hae*III endonuclease restriction fragments on electrophoretic migration can be seen in Figure 3(a). Distamycin and **1** bring about much smaller mobility changes (data not shown). Compound **18**, essentially the polyamine moiety of **4**, also produces little apparent change in electrophoretic behavior compared with the control lane (data not shown).

The electrophoretic mobilities of the ϕX-174 DNA digested with *Hae*III endonuclease restriction fragments in the presence of **4** may be expressed as R_L values [R_L is the ratio of the apparent length to real length where apparent length is the length of uncomplexed dsDNA (interpolated or slightly extrapolated from the standards) with the same mobility].[15] The plot of R_L for the 1078 bp fragment versus concentration of **4** in Figure 3b(b) shows that influence of **4** on the DNA conformation is nearly linearly dependent on the

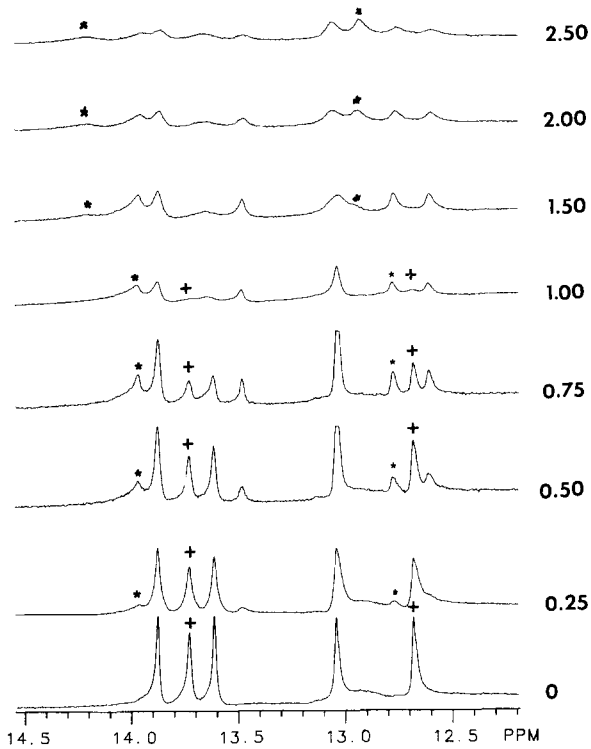

Figure 2. Titration of a solution 1 mM in d(CGCAAATTTGCG)$_2$. 10 mM phosphate buffer (pH 7.0) with **4** in H_2O:D_2O 9:1 at 25 °C at the indicated mol ratios of **4**/dsDNA. The binding of **4** was followed by the disappearance of the resonances marked with plus (+) signs and the appearance of the resonances marked with asterisks (*) in the titration spectrum.

concentration of **4** until saturation by 4 at ca. 40 μM. This contrasts to **6a**'s sigmoidal dose response in that the change in R_L with **6a** is not as great at saturation which is at concentrations of **6a** greater than 50 mM.

Discussion

^{1}H NMR titration

Previous ^{1}H NMR studies of the structures of complexes of dien-microgonotropen (**5c**), tren-microgonotropen (**6b**), and the Zn^{2+} ligated **6b** with d(CGCAAATTTGCG)$_2$ lead to the determination of their solution structures. In the present instance, due to the symmetrical appearance of —CH_2—CH_2—NH— building units it is not possible to obtain unambiguous assignments of the methylene signals such that a solution structure by NOESY experiments was not possible. The present ^{1}H NMR titration had two purposes: (1) to show which bases are involved in the minor groove binding of the tripyrrole peptide moiety, (2) establish stoichiometry of complexes and (3) to determine the existance of interactions of the polyamine substituent with the phosphate backbone as well as its orientation.

The titration of d(CGCAAATTTGCG)$_2$ with **4** in H_2O:D_2O 9:1 shows that there is a 2:1 asymmetric type of binding of **4** to dsDNA. It was shown that **6b** also forms a 2:1 complex[7b] [ca. 15% at 2:1 **6b**/d(CGCAAATTTGCG)$_2$]. The binding occurs in the A•T-rich region, as in the case of distamycin[11] and microgonotropens,[7] and as a result there are extensive line broadenings in this region. The fraying of the ends of the dsDNA is diminished upon reaching the 2:1 **4**/dsDNA mol ratio at which point the terminal G•C imino signals sharpen compared with the A•T imino signals. Several explanations for the finding of relatively sharp G•C imino signals compared with the A•T imino signals can be considered. One is that there could be stiffening of the dsDNA due to binding of the tripyrrole peptide moiety into the minor groove of the dsDNA. Another possibility is that the polyamine chain covers the phosphate backbone and reaches the terminal G•C base pairs. Although stabilization of dsDNA could occur upon ligand binding, we did not see any stiffening of the end base pairs when studying

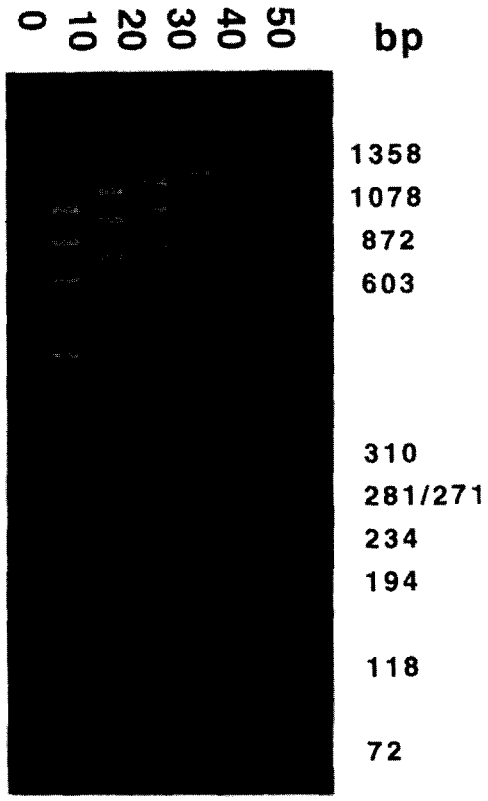

Figure 3a. (a) Effect of ligand binding on the electrophoretic mobility of ϕX-174 DNA digested with endonuclease restriction fragments (sizes indicated to the right side of the figure). Lanes 1–6 have the indicated concentrations (in μM) of **4** (0 is control DNA restriction fragments with no added agents).

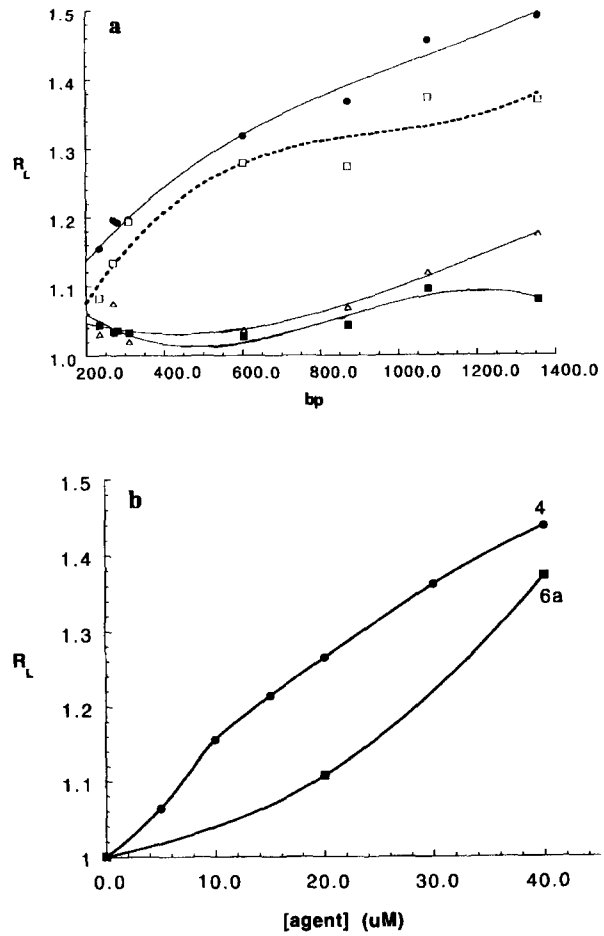

Figure 3b. (a) A plot of the ratio of apparent DNA length to real length (R_L) versus the number of base pairs (bp) in the longest and intermediate sized DNA fragments in the presence of 40 μM **4** (●), 40 μM **6a** (□), 150 μM **Dm** (■) and 150 μM **18** (Δ). The curves are interpolations between the data points for **4**. (b) Employing the 1078 bp DNA fragment plot of the ratio of apparent DNA length to real length (R_L) versus [agent] [**4** (●), **6a** (◆)]. The curves are interpolations between the data points for **4** and **6a**. The data for Figure 3(b) was generated from Figure 3(a) and previously collected data 3d as explained in the text.

the same dsDNA when complexed to **5c**, **6b** and distamycin.[11] There were always broad G•C end imino signals that sharpen only on cooling at −5 and −10 °C.[11] Therefore, the only factor that can contribute to the stiffening of the end base pairs is the interaction of the polyamine moiety with the phosphate backbone running down to the end G•C base pairs. The loss in intensities of the NMR signals as the titration approaches the 2:1 ratio is due to the partial precipitation of the **4**-dsDNA complex. Presumably this is due to the neutralization of the phosphate oxygen's charges as they pair with the protonated polyamine moiety of **4**. This in turn is indicative of the electrostatic interaction of the polyamine substituent with the phosphate backbone. It would appear, therefore, that the amino groups of the side chain of **4** do not extend out into solution. The 2:1 asymmetric binding mode was confirmed by the titration in D_2O.

The difference in structure between **4** and the previously investigated **6b** resides in the polyamine moiety attached to the central pyrrole ring. In contrast to **6b**, the polyamino substituent of **4** lifts the tripyrrole peptide in the minor groove. This may assist quantitative formation of the 2:1 complex with **4**.[11,12] The stiffening of the end base pairs, as well as the difference in the chemical shifts in the G•C imino signals, show that the polyamine moiety of **4** orients towards the end base pairs in its 2:1 complex and not towards the central A•T-rich region. This behavior will lead to more coverage of the phosphate oxygens (the A•T-rich region by the tripyrrole peptide and partly by the polyamine moiety, and the G•C-rich region by the polyamine moiety and the dimethylamine substituent R3) and also to less bulkiness of the central dsDNA unit where **4** binds. However, the length of the polyamine moiety wrapping the phosphate backbone brings a certain asymmetry in the 2:1 binding mode.

Equilibrium constants for the association of 4 with hexadecameric duplex d(GGCGCA$_3$T$_3$GGCGG)/ d(CCGCCA$_3$T$_3$GCGCC)

Several conclusions concerning microgonotropen minor groove binding agents (tripyrrole peptides) can be made by a comparison of the equilibrium association constants found in Table 2. Substituting the amino terminal formyl group of distamycin with an acetamido and the carboxy terminal amidine with $-CH_2CH_2$-$CH_2(NCH_3)_2$ yields compound **2** along with a 3 order of magnitude decrease in binding affinity ($K_{L1}K_{L2}$) compared to distamycin (1.0×10^{16} M^{-2}). Changing the *N*-methyl group on the central pyrrole of **2** to an *N*-pentaazapentabutylamino functionality **4** more than compensates for **2**s decrease in binding affinity (it increases by ca. 25,000-fold). The protonated *N*-propylamine of the central pyrrole of **1** is able to electrostatically interact with the DNA's phosphates' oxyanions while an *N*-methyl group of **2** only provides van der Waals interactions with the walls of the minor groove. Adding three appropriate amines (that are likely protonated under neutral conditions) separated by methylene linkers to the *N*-propylamine moiety of **1** yields **6a** and an increase in $K_{L1}K_{L2}$ over that seen with **1** of 2 orders of magnitude. Changing the linker on the nitrogen of the central pyrrole unit of **1** from *N*-propyl amine to *N*-butyl amine provides **6b** and an increase in $K_{L1}K_{L2}$ over that seen in **1** of 1.5 orders of magnitude. Adding the pentaaza pentabutylamine to **1** provides an increase in $K_{L1}K_{L2}$ of 1 order over that for **1**. The polyamines are protonated under neutral conditions and held firmly on the phosphate backbone by electrostatic enforced hydrogen bonding.[19] Compound **6a** has an increase in $K_{L1}K_{L2}$ of 1 order magnitude and **6b** has an increase of 0.5 order of magnitude over **4**. The tris(2-aminoethyl) amino moiety of **6a** and **b** sequesters two of the DNA's phosphodiester groups.[3d] The solution structure of the 1:1 complex of dsDNA with **6b** has been determined earlier by 2-D NMR spectroscopy (NOESY).[7b] The pentaaza pentabutylamine moiety of **4** lays on the phosphodiester backbone and orients itself towards the end base pairs of hexadecameric duplex DNA, as is evident from the results of ^{1}H NMR titration of dsDNA with **4**. In Figure 4 we depict an energy minimized plausible structure which exhibits the characteristics that we have enumerated. Microgonotropen **4** is third in its affinity for dsDNA in the series for $K_{L1}K_{L2}$, where **6a** > **6b** > **4** = **5a** > **5b** > **5c** > **1** > distamycin >> **2**.

Electrophoretic mobility shift assay

Employment of ϕX-174 DNA digested with *Hae*III endonuclease is predicated on its use as a DNA molecular weight size standard and its slight A+T-richness (55%).[13] There are 246 A-tracts (AAAA, AAAT or TAAA; independent or overlapping) that are the most preferred binding sites for distamycin and its analogues. These sites are approximately evenly distributed and separated on the average by ca. 29±14 bp. This frequency is common to fragments of all sizes. With increasing concentrations of the microgonotropens, the electrophoretic mobility of the DNA restriction fragments decreases. The decrease in mobility is most pronounced for the largest restriction fragments and not perceptible for the smallest. This suggests that the binding of the microgonotropens to A+T-rich sites changes the DNA conformation at these sites and that a critical number of sites are required before conformational changes manifest themselves by influencing the electrophoretic mobility. Complexing of **4** to DNA results in the interaction of the positive charges of the protonated microgonotropen' polyamine moieties with the negatively charged phosphate backbone. The resultant decrease in the net negative charge alone does not provide an explanation for the decrease in electrophoretic mobility. This is so, since the shortest fragments would be expected to exhibit the greatest change in mobility (at a constant charge to mass ratio, electrophoretic mobility is an approximately logarithmic function of mass). Instead, it is the longest fragments (1358, 1078 and 872 bp) whose mobility shows the greatest change. A 'smearing' of the bands is evident in the intermediate sized fragments

(603, 310, 281/271 and 234 bp), above 30 mM of **4**. This indicates not simply a conformational change, but a population of differing conformations of DNA•microgonotropen complexes leading to a distribution of apparent electrophoretic molecular weights and, hence, less sharply defined bands. This differing response of electrophoretic mobility to microgonotropen concentration is not due simply to the relative affinities of the different microgonotropens (log $K_{L1}K_{L2}=17.4$ for **4** and 18.4 for **6a**; Table 2). This suggests that the mode of inhibition of DNA mobility in an electrophoretic field is not simply a function of how tight a ligand binds to the DNA. Instead, the degree of inhibition is likely due to a less tangible quality of the microgonotropen which induces a DNA conformational change upon association. Alteration of DNA conformation by **6b** has been verified by atomic force microscopy.[14] Distamycin and **18** do not demonstrate very marked changes even at the 150 mM. As is evident from the above discussion, **4** is much more effective in inducing structural changes than are the sum of its parts. Of the microgonotropens investigated to date **6a** has the greatest constants for complementary binding to dsDNA while at concentrations below 40 μM **4** has the greatest influence upon dsDNA conformation.

Experimental

Synthetic materials

Reagent grade chemicals were used without further purification unless otherwise stated. Triethylamine and pyridine were dried over KOH and distilled. Methylene chloride was distilled over P_2O_5. Anhydrous DMF, 4-amino-1-butanol, benzyl chloroformate, di-*tert*-butyl dicarbonate, Tosyl chloride, DCC, pyridinium dichromate and 1-hydroxy benztriazole (HOBT) were purchased from Aldrich. After treatment with 0.5 M KOH, Dowex ion-exchange resin (Aldrich) was washed with distilled water and methanol before using.

Synthetic methods

IR spectra were obtained neat on a Matteson Genesis Series FT IR. ^{1}H NMR spectra were recorded on a Gemini-200 (Varian) or a General Electric GN-500 spectrometer using $CDCl_3$ or DMSO-d_6. Chemical shifts are reported in δ (ppm) relative to $CHCl_3$ (7.24 ppm) or DMSO-d_6 (2.49 ppm), coupling constants are reported in Hz. DFQ-COSY spectra were recorded on a GN-500 spectrometer in 4 K complex points for 411 t_1 increments with a spectral width of 6024 Hz in both

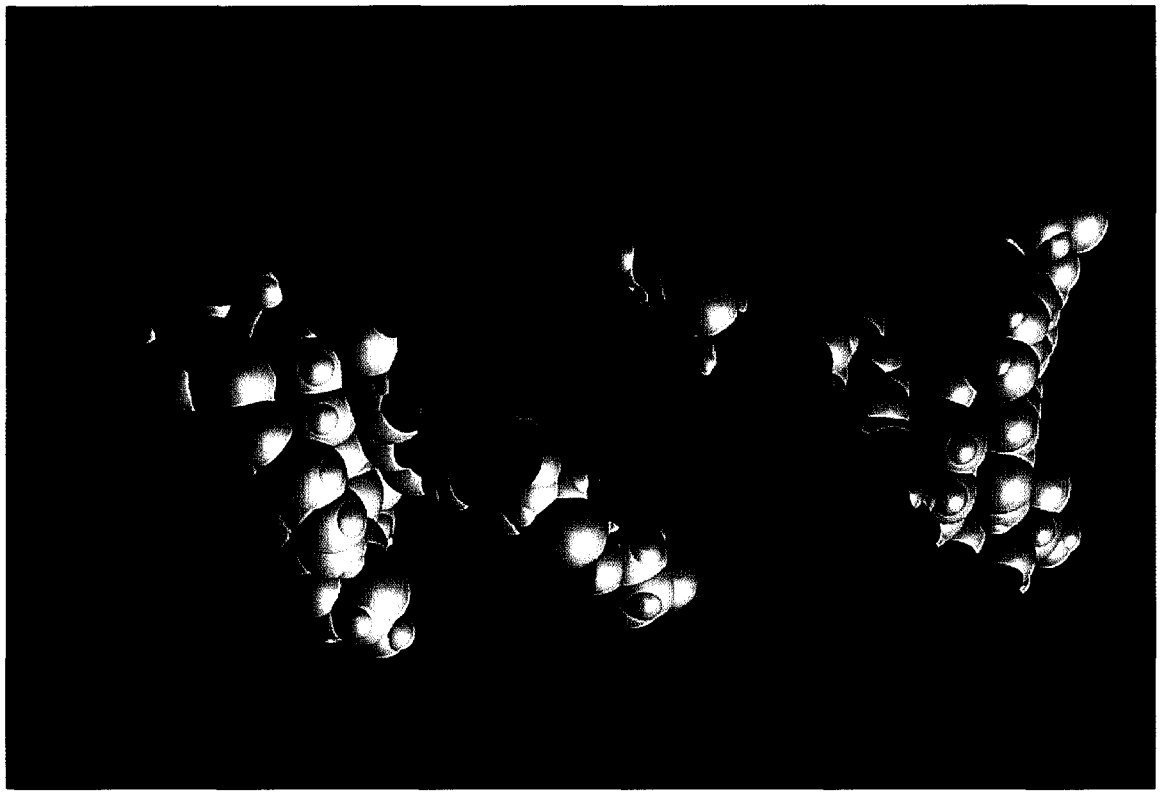

Figure 4. An energy minimized (CHARMm[20]) plausible structure that depicts the salient features of the 2:1 complex of **4**: $(CGCAAATTTGCG)_2$. ^{1}H NMR titration experiments and accompanying chemical shifts show the two tripyrrole peptide moieties bind in the minor groove in the A•T rich region of dsDNA, while the polyamine substituents lie along the phosphate backbone, reaching the terminal residues and stiffening the ends of the dodecamer. The observed stiffening of the terminal base pairs as well as the difference in the G•C imino chemical shifts show that the polyamine moiety of **4** is oriented towards the ends of the dodecamer and not towards the central A•T rich region. This orientation leads to a more complete binding to the phosphate oxygens and to less steric conflicts in the central A_3T_3 region where **4** binds. The protonated amine functions are assumed to complex in pairs to the phosphate linkages as was shown in the 2-D NMR structures of **6b** with dsDNA.[7b] The length of the polyamine moiety binding along the phosphate backbone brings an asymmetry to the 2:1 binding mode.

dimensions. The data matrix was zero filled to 2 K and appodized with a double exponential function to give a line broadening of 1 Hz in both frequency domain. Low-resolution mass spectra [EI and low-resolution FAB (using NBA matrix)] were recorded on a VG-70 E double focusing mass spectrometer with VG-Opus/Cios data system interface. High-resolution mass spectrometry was performed at the Mass Spectrometry Facility, Department of Chemistry and Biochemistry, University of California, Los Angeles, using the FAB technique and NBA matrix. Chromatographic silica gel (ICN Silica 32–60, 60 A) was used for flash chromatography and glass backed plates of 0.25 mm Silica Gel 60-F_{254} (Merck) were used for TLC.

4-(Benzyloxycarbonyl) amino-1-butanol (8). To a cooled solution (ice bath) of Na_2CO_3 (49.3 g, 0.45 mol) in distilled water (200 mL) was added 4-amino-1-butanol (20.0 g, 0.22 mol). Benzyl chloroformate (57.3 g, 0.37 mol) was added slowly while stirring. The mixture was stirred (ice bath) for 2 h and continued stirring overnight at room temperature. The product crystallized out of the solution, was filtered and recrystallized from EtOAc to obtain the pure carbamate **8**, 40.2 g (80%), as white crystals: mp 80–81 °C; ^{1}H NMR ($CDCl_3$): δ 1.55–1.61 (m, 4H, —CH_2—CH_2—), 3.22 (t, J=6.3 Hz, 2H, —NH—CH_2—), 3.65 (t, J=5.98 Hz, 2H, —CH_2—OH), 5.08 (s, 2H, —OCH_2—Ar), 7.34–7.36 (m, 5H, ArH); IR (film): 3322, 2944, 1681, 1531, 1457, 1336, 1268, 1234, 1056, 1008 cm^{-1}; MS (EI) *m/e* relative abundance) 223 (M^+, 25), 108 ($M^+ - C_5H_{10}O_2N$, 45), 91($M^+ - C_5H_{10}O_3N$, 100).

4-(Benzyloxycarbonyl) amino butyl-1-*p*-toluenesulfonate (9). To a solution of **8** (38.7 g, 0.17 mol) in pyridine (250 mL) was added *p*-toluenesulfonyl chloride (49.1 g, 0.26 mmol) at 0–5 °C. The mixture was stirred (ice bath) for 3 h, poured in ice water and acidified with concd HCl. The tosylate crystallized out of the solution and was filtered. It was recrystallized from ethyl acetate to give pure **9**, 58.8 g (91%), mp 46–48 °C; ^{1}H NMR ($CDCl_3$): δ 1.48–1.70 (m, 4H, —CH_2—CH_2—), 2.43 (s, 3H, Ar—CH_3), 3.13 (m, 2H, —NH—CH_2), 4.02 (t, J=6.1 Hz, 2H, —CH_2—OTs), 4.73 (br, 1H, —NH—), 5.06 (s, 2H, —OCH_2—Ar), 7.30–7.33 (m, 7H, ArH), 7.76 (d, J=8.3 Hz, 2H, ArH); IR (film): 2950, 1710, 1527, 1452, 1353, 1249, 1176, 948 cm^{-1}; MS (EI) *m/e* (relative abundance) 377 (M^+, 20), 205 ($M^+ - C_7H_7O_3S$, 10), 108 ($M^+ - C_{12}H_{16}NO_4S$, 20), 91 ($M^+ - C_{12}H_{16}NO_5S$, 100).

5-*tert*-Butyloxycarbonyl-10-benzyloxycarbonyl-5,10-diaza-1-decanol (10). A solution of **9** (58.8 g, 0.15 mol) and 4-amino-1-butanol (16.7 g, 0.18 mol) in DMF (70 mL) was stirred at 90 °C for 1.5 h. Cooled to room temperature and poured into ice water (140 mL). The solution was made alkaline (pH 12) by adding aqueous 5% KOH solution and extracted with CH_2Cl_2 (3 × 100 mL). The combined organic layer was washed with brine (1 × 100 mL), dried (Na_2SO_4) and the solvent was removed under reduced pressure. The residue was purified by chromatography (silica, 5% MeOH–CH_2Cl_2, then CH_2Cl_2–MeOH–Et_3N, 17:2:1) to give **10**, 28.9 g (63%) as a clear viscous oil. ^{1}H NMR ($CDCl_3$): δ 1.48–1.61 (m, 8H, —CH_2—CH_2—), 2.57–2.62 (m, 4H, —CH_2—NH—CH_2—), 3.13–3.17 (m, 2H, —CH_2—NHCO—), 3.52 (t, J=5 Hz, 2H, —CH_2—OH), 5.05 (s, 2H, —OCH_2Ar), 7.31–7.33 (m, 5H, ArH); IR (film) 3307, 2935, 1700, 1538, 1456, 1259, 1137, 1054, 775, 698 cm^{-1}; MS (EI) *m/e* (relative abundance) 294 (M^+, 10), 235 ($M^+ - CHO_2N$, 8), 91 ($M^+ - C_9H_{19}N_2O_3$, 100).

5-*tert*-Butyloxycarbonyl-10-benzyloxycarbonyl-5,10-diazadecyl-1-*p*-toluenesulfonate (11). To a solution of **10** (26.8 g, 91 mmol) in CH_2Cl_2 (240 mL) was added dropwise di-*tert*-butyl dicarbonate (21.8 g, 99.8 mmol) at 0–5 °C. The mixture was stirred for 30 min and the solvent removed under reduced pressure. The residue was dissolved in pyridine (150 mL) and *p*-toluenesulfonyl chloride (27.19 g, 0.14 mol) was added at 0–5 °C. The mixture was stirred in the cold condition for 3 h, poured in ice water (200 mL) and extracted with CH_2Cl_2 (3 × 100 mL). The combined organic layer was dried (Na_2SO_4) and solvent removed under reduced pressure. The crude product was purified by chromatography (silica, 20% EtOAc–CH_2Cl_2) to give **11**, 33.2 g (66%). ^{1}H NMR ($CDCl_3$): δ 1.39 [s, 9H, —$C(CH_3)_3$)], 1.41–1.59 (m, 8H, —CH_2—CH_2—), 2.42 (s, 3H, $ArCH_3$), 3.07–3.20 [m, 6H, —CH_2—N(Boc)—CH_2— and —NH—CH_2—], 4.00 (t, J=5.9 Hz, 2H, —CH_2—OTs), 5.07 (s, 2H, —OCH_2—Ar), 7.29–7.34 (m, 7H, ArH), 7.76 (d, J=8.3 Hz, 2H, ArH); IR (film): 2940, 1693, 1531, 1469, 1365, 1255, 1174, 1033, 817 cm^{-1}; LRMS (FAB) *m/e* 549 ($M+H^+$).

10-*tert*-Butyloxycarbonyl-15-benzyloxycarbonyl-5,10,15-triaza-1-pentadecanol (12). Same general procedure as **10**. Yield, 16.7 g (60%); ^{1}H NMR ($CDCl_3$): δ 1.41 [s, 9H, —$C(CH_3)_3$], 1.47–1.65 (m, 12H, —CH_2—CH_2—), 2.54–2.63 (m, 4H, —CH_2—NH—CH_2—), 3.10–3.21 [m, 6H, —CH_2—N(Boc)— and —NH—CH_2—], 3.53 (t, J=5.4 Hz, 2H, —CH_2—OH), 5.07(s, 2H, —OCH_2—Ar), 7.33–7.35 (m, 5H, ArH); IR (film): 3330, 2971, 2863, 1693, 1536, 1419, 1365, 1259, 1168, 736 cm^{-1}; MS (EI) *m/e* (relative abundance) 465 (M^+, 10), 102 ($M^+ - C_{20}H_{33}N_3O_3$, 100), 91 ($M^+ - C_{18}H_{36}N_3O_5$, 97).

5,10-Di-*tert*-butyloxycarbonyl-15-benzyloxycarbonyl-5,10,15-triazapentadecyl-1-*p*-toluenesulfonate (13). Same general procedure as **11**. Yield, 11.7 g (45%); ^{1}H NMR ($CDCl_3$): δ 1.40 [s, 18H, —$C(CH_3)_3$], 1.41–1.60 (m, 12H, —CH_2—CH_2—), 2.43 (s, 3H, $ArCH_3$), 3.12–3.21 [m, 8H, —CH_2—N(Boc)—CH_2], 4.00 (t, J=6.04 Hz, 2H, —CH_2—OTs), 5.07 (s, 2H, —OCH_2—Ar), 7.31–7.34 (m, 7H, ArH), 7.76 (d, J=8.26 Hz, 2H, ArH); IR (film): 2973, 1691, 1477, 1419, 1365, 1255, 1174, 736 cm^{-1}; LRMS (FAB) *m/e* 720 ($M+H^+$).

10,15-Di-*tert*-butyloxycarbonyl-20-benzyloxycarbonyl-5,10,15,20-tetraaza-1-icosanol (14). Same general procedure as **10**. Yield, 5.6g (56%); ^{1}H NMR ($CDCl_3$): δ 1.42 [s, 18H, —$C(CH_3)_3$], 1.47–1.64 (m, 16H, —CH_2—CH_2—), 2.57–2.64 (m, 4H, —CH_2—NH—CH_2—), 3.12–3.22 [m, 8H, —CH_2—N(Boc)—CH_2], 3.55 (m, 2H, —CH_2—OH), 5.07 (s, 2H, —OCH_2—Ar), 7.32–7.35 (m, 5H, ArH); IR (film): 3332, 2933, 28.65, 1679, 1479, 1419, 1365, 1255, 1166, 736 cm^{-1}; LRMS (FAB) *m/e* 637 ($M+H^+$).

5,10,15-Tri-*tert*-butyloxycarbonyl-20-benzyloxycarbonyl-5,10,15,20-tetraazaicosyl-1-*p*-toluenesulfonate (15). Same general procedure as **11**. Yield, 3.7 g, (48%); ^{1}H NMR ($CDCl_3$): δ 1.42 [s, 27H, —$C(CH_3)_3$], 1.40–1.62 (m, 16H, —CH_2—CH_2—), 2.43 (s, 3H, $ArCH_3$), 3.04–3.22 [m, 12H, —CH_2—N(Boc)—CH_2], 4.01 (t, $J=6.03$ Hz, 2H, —CH_2—OTs), 5.07 (s, 2H, —OCH_2—Ar), 7.31–7.34 (m, 7H, ArH), 7.76 (d, $J=8.3$ Hz, 2H, ArH); IR (film): 2973, 2933, 1687, 1479, 1419, 1365, 1280, 1174, 736 cm^{-1}; LRMS (FAB) *m/e* 891 ($M+H^+$).

10,15,20-Tri-*tert*-butyloxycarbonyl-25-benzyloxy-carbonyl-5,10,5,20,25-pentaaza-1-pentacosanol (16). Same general procedure as **10**. Yield, 2.1g, (64%); ^{1}H NMR δ 1.42 [s, 27H, —$C(CH_3)_3$], 1.43–1.66 (m, 20H, —CH_2—CH_2—), 2.60–2.65 [m, 12H, —CH_2—N(Boc)—CH_2], 3.53–3.58 (m, 2H, —CH_2—OH), 5.07 (s, 2H, —OCH_2—Ar), 7.32–7.34 (m, 5H, ArH); IR (film): 3440, 3351, 2935, 2865, 1679,, 1536, 1479, 1419, 1390, 1164 cm^{-1}; LRMS (FAB) *m/e* 808 ($M+H^+$).

5,10,15,20-Tetra-*tert*-butyloxycarbonyl-25-benzyloxy-carbonyl-5,10,15,20,25-pentaaza-1-pentacosanoic acid (17). To a solution of **16** (500 mg, 0.62 mmol) in CH_2Cl_2 (5 mL) was added di-*tert*-butyl dicarbonate (142 mg, 0.65 mmol) at 0–5 °C. The reaction was stirred for 20 min and the solvent removed under reduced pressure. The residue was dissolved in DMF (5 mL) and PDC (1.16 g, 3 mmol) was added. The mixture was stirred for 4 h at room temperature, poured into ice water (20 mL) and extracted with ether (3 × 10 mL). The combined organic layer was washed with water (2 × 10 mL), dried (Na_2SO_4) and the solvent removed. The residue was purified by chromatography (silica, 30% EtOAc–CH_2Cl_2, then 5% MeOH–CH_2Cl_2) to give **17**, 194 mg (35%). ^{1}H NMR ($CDCl_3$): δ 1.42 [s, 36H, —$C(CH_3)_3$], 1.36–1.52 (m, 20H, —CH_2—CH_2—), 3.07–3.24 [m, 16H, —CH_2—N(Boc)—CH_2], 5.07 (s, 2H, —OCH_2—Ar), 7.32–7.34 (m, 5H, ArH); IR (film): 3323, 2972, 2247, 1678, 1475, 1420, 1367, 1249, 1164, 913 cm^{-1}; LRMS (FAB) *m/e* 922 ($M+H^+$).

Compound (19). To a solution of pentamer acid **17** (182 mg, 0.19 mmol), microgonotropen **1** (131 mg, 0.23 mmol), HOBT (36 mg, 0.26 mmol) in DMF (1.5 mL) was added DCC (51 mg, 0.24 mmol). The reaction was stirred at room temperature for 46 h, filtered and the solvent removed under reduced pressure. The residue was purified by chromatography (silica, CH_2Cl_2:MeOH:Et_3N, 17:2:1) to give **19**, 189 mg (55%). ^{1}H NMR (DMSO-d_6): δ 1.36 [s, 36H, —$C(CH_3)_3$], 1.38 (m, 16H, —CH_2—CH_2—) 1.64 (m, 2H, —CH_2CH_2CONH), 1.80 (m, 2H, —CH_2NHCO), 1.97 (s, 3H, —$COCH_3$), 2.18 (s, 6H, $N(CH_3)_2$), 2.30 [t, $J=7$ Hz, 2H, —$CH_2N(CH_3)_3$], 2.99 (m, 2H, —CH_2NHCbz), 3.08 [m, 16H, —CH_2—N(Boc)—CH_2], 3.18 (m, 2H, $CONHCH_2$), 3.79, 3.82 (2s, 6H, pyrrole N—CH_3), 4.30 (t, $J=2.6$ Hz, 2H, pyrrole N—CH_2), 4.99 (s, 2H, —OCH_2—Ar), 6.82 (d, $J=0.4$ Hz, 1H, pyrrole ArH), 6.86 (s, 1H, pyrrole ArH), 7.02 (s, 1H, pyrrole ArH), 7.14 (d, $J=0.6$ Hz, 1H, pyrrole ArH), 7.18 (s, 1H, pyrrole ArH), 7.29–7.36 (m, 5H, ArH), 7.80 (t, $J=2.2$ Hz, 1H, —NHCO), 8.05 (t, $J=2.2$ Hz, 1H, —NHCO—), 9.81 (s, 1H, Pyr—CONH—Pyr), 9.89, (2s, 2H, Pyr—CONH—Pyr); IR (film): 2927, 1662, 1552, 1465, 1415, 1365, 1255, 1164 cm^{-1}; HRMS (FAB) *m/e* 1457.9136 (calcd for $C_{75}H_{121}N_{14}O_{15}$ ($M+H^+$) 1457.9135).

Compound (4). A solution of **19** (105 mg) in MeOH (3.5 mL) was stirred in hydrogen atmosphere for 3 h with 10% Pd–C catalyst (35 mg). The slurry was filtered through celite and solvent removed under reduced pressure. The residue was dissolved in CH_2Cl_2 (3 mL), cooled to 0–5 °C and TFA (2 mL) was added dropwise. The reaction was stirred for 20 min and solvent removed under reduced pressure. The residue was dissolved in MeOH (40 mL) stirred with Dowex 1 × 8 ion-exchange resin (OH form) in room temperature for 30 min. The resin was removed by filtration and the filtrate was evaporated to afford **4** (49 mg, 74%) as a slightly yellowish oil. ^{1}H NMR: refer to Table 1; IR (film): 3401, 2364, 1579, 1475, 1421, 1170, 1041, 858, 746 cm^{-1}; HRMS (FAB) *m/e* 923.6653 (calcd for $C_{47}H_{83}N_{14}O_5$ ($M+H^+$) 923.6670).

5,10,15,20,25-Pentaaza-1-pentacosanol (18). Same as **4**. Yield 95%; ^{1}H NMR ($CDCl_3$): δ 1.45–1.66 (m, 20H, —CH_2—), 2.46–2.72 (m, 18H, —CH_2—NH—CH_2—), 3.55 (t, $J=5.4$ Hz, 2H, —CH_2OH); IR (film): 3384, 1643, 1563, 1481, 1432, 1386, 1319, 1126 cm^{-1}; LRMS (FAB) *m/e* 374 ($M+H^+$).

Reagents and methods for DNA binding studies

The complementary hexadecameric oligonucleotides d(GGCGCAAATTTGGCGG) and d(CCGCCAAATTTGCGCC) were synthesized at UCSF's Biomolecular Resource Facility. Annealing and characterization procedures for the duplex hexadecamer have been described.[9,3d] Hoechst 33258 (Aldrich) was used without further purification. The duplex hexadecamer was maintained in a stock solution containing 0.01 M potassium phosphate buffer, pH 7.0, 0.01 M NaCl. All other stock solutions were in distilled deionized water. Stock solutions were stored on ice for the duration of a given experiment and maintained at −20 °C between

experiments. In all fluorescence titrations, solutions were buffered with 0.01 M potassium phosphate buffer, pH 7.0, 0.01 M KCl ($\mu = 0.028$; filtered through a sterile 0.2 μ Nalgene disposable filter). The final concentration of duplex hexadecamer was always 5.0×10^{-9} M. The concentrations of **4** used were 3.0×10^{-9}, 5.0×10^{-9}, 6.0×10^{-9}, 7.5×10^{-9}, 9.0×10^{-9} and 1.0×10^{-8} M. Buffered solutions (2.8 mL) containing dsDNA ± **4** were titrated with a 3.5×10^{-6} M solution of Hoechst 33258 (**Ht**) until a final concentration of 1.8×10^{-7} M was reached. All titration volumes were measured with Gilson Pipetman microliter pipets and disposable pipet tips. The solutions were excited at 354 nm and fluorescence emissions were measured at 450 nm using the mean value of triplicate data collections with a thermostated (35 °C) Perkin–Elmer LS-50 fluorescence spectrophotometer. The samples were continuously stirred in matched quartz cuvettes (1 cm path length) and allowed at least 2 min to equilibrate between each titrant addition and fluorescence recording. The cuvettes were washed exhaustively with 10% HNO_3 and rinsed ≥5 times with distilled deionized H_2O before drying and subsequent use. Background fluorescence intensity (buffered solution of hexadecamer before the addition of any **Ht**) was subtracted from each titration point to provide the corrected fluorescence intensity, F. These corrected fluorescence intensity data points were fit to theoretical curves based on equation (1) with SigmaPlot 4.1.4 (Jandel Scientific) on a Macintosh Quadra 800 computer. Since the total fluorescence (SF) varied slightly from one experiment to the next, this value was determined for each experiment (ca. 70 fluorescence units) from a titration of the dsDNA with **Ht** in the absence of any added ligand.

^{1}H NMR titration

All NMR experiments were performed on a GE-500 spectrometer at 500.125 MHz at 25 °C. The titration in H_2O:D_2O 9:1 was recorded using a **1331** pulse sequence.[16]

Electrophoretic mobility assay

The final concentrations (10 μL) of all reactions were 0.15 mg/mL ϕX-174 DNA digested with *Hae*III endonuclease (Pharmacia) in 10 mM Tris-HCl, pH 7.5, 50 mM KCl. Incubation of the DNA with compounds that could potentially alter DNA conformation [at 5, 10, 15, 20, 25, 30, 40, 50 μM, **6a** at 20, 40, 60 or 80 μM (from previously performed experiments);[3d] **Dm** (Sigma) and **18** at 150 mM] was for 60 min at room temperature (control reactions were exactly the same except that additional agents were not added). At this time, 1.1 μL of 10% (w/v) glycerol, 0.1% (w/v) sodium dodecyl sulfate and 0.1% (w/v) bromophenol blue loading buffer[17] was added to each sample. Samples were electrophoretically separated through a 4% NuSieve 3:1 agarose (FMC) gel in 40 mM Tris-acetate, 0.2 mM EDTA, pH 7.8 (1× TAE)[17] for 4.0 h at 3 V/cm (after pre-electrophoresis of the gel for 0.5 h). The gels were stained with a 0.5 μg/mL solution of ethidium bromide in deionized water for 30 min, destained for 15 min in deionized water and photographed on a UV (302 nm) transilluminator with Polaroid type 667 film.

Molecular modeling was performed on a Silicon Graphics (Mountain View, CA) Iris4D/340GTX workstation in the graphics program QUANTA[20] (Version 4.0). The structure of **6b** complexed to $d(CGCAAATTTGCG)_2$[7b] was used as the initial coordinates for construction of **4**. The methylene chain and the tren polyamino moiety on the central pyrrole nitrogen of **6b** were replaced with R2 and R4 using 3D Molecular Editor (QUANTA). The partial atomic charges of the atoms in **4** and $d(CGCAAATTTGCG)_2$ were generated from the CHARMm force-field parameter files. Minimization was performed as described previously in CHARMm[20] (Version 22 interface).

Acknowledgement

We express appreciation to the Office of Naval Research for a grant (N000 14–90-J-4132) to support this work.

References

1. (a) Beerman, T. A.; McHugh, M. M.; Sigmund, R.; Lown, J. W.; Rao, K. E.; Bathini, Y. *Biochim. Biophys. Acta* **1992**, *1131*, 53; (b) Boger, D. L.; Sakya, S. M. *J. Org. Chem.* **1992**, *57*, 1277; (c) Lown, J. W.; Krowicki, K.; Bhat, U. G.; Skorobogaty, A.; Ward, B.; Dabrowiak, J. C. *Biochemistry* **1986**, *25*, 7408; (d) Nunn, C. M.; Jenkins, T. C.; Neidle, S. *Biochemistry* **1993**, *32*, 13838.

2. (a) Kopka, M. L.; Yoon, C.; Goodsell, D.; Pjura, P.; Dickerson, R. E. Proc. *Natl. Acad. Sci. U.S.A.* **1985**, *82*, 1376; (b) Coll, M.; Frederick, C. A.; Wang, A. H.-J.; Rich, A. *Proc. Natl. Acad. Sci. U.S.A.* **1987**, *84*, 8385; (c) Teng, M.-K.; Usman, N.; Frederick, C. A.; Wang, A. H.-J. *Nucl Acids Res.* **1988**, *16*, 2671; (d) Carrondo, M. A. A. F. de C. T.; Coll, M.; Aymami, J.; Wang, A. H.-J.; van der Marel, G. A.; van Boom, J. H.; Rich, A. *Biochemistry* **1989**, *28*, 7849; (e) Scahill, T. A.; Jensen, R. M.; Swenson, D. H.; Hatzenbuhler, N. T.; Petzold, G. L.; Wierenga, W.; Brahme, N. M. *Biochemistry* **1990**, *29*, 2852; (f) Chen S.-M.; Leupin, W.; Rance, M.; Chazin, W. J. *Biochemistry* **1992**, *31*, 4406; (g) Edwards, K. J.; Jenkins, T. C.; Neidle, S. *Biochemistry* **1992**, *31*, 7104.

3. (a) Bruice, T. C.; Mei, H.-Y.; He, G.-X.; Lopez, V. *Proc. Natl. Acad. Sci. U.S.A.* **1992**, *89*, 1700; (b) Browne, K. A.; Bruice, T. C. *J. Am. Chem. Soc.* **1992**, *114*, 4951; (c) He, G.-X.; Browne, K. A.; Groppe, J. C.; Blaskó, A.; Mei, H.-Y.; Bruice, T. C. *J. Am. Chem, Soc.* **1993**, *115*, 7061; (d) He, G.-H.; Browne, K. A.; Blaskó, A.; Bruice. T. C. *J. Am. Chem. Soc.* **1994**, *116*, 3716.

4. Xue, T.; Browne, K. A.; Bruice, T. C. *Bioconj Chem.* **1995**, *6*, 82.

5. (a) Corey, E. J.; Schmidt, G. *Tetrahedron Lett.* **1979**, 399; (b) Sasaki, N. A.; Hashimoto, C.; Potier, P. *Tetrahedron Lett.* **1987**, 6069.

6. Maryanoff, B. E.; Greco, M. N.; Zhang H.-C.; Andrade-Gordon, P.; Kauffman, J. A.; Nicolau, K. C.; Liu, A.; Brungs, P. H. *J. Am. Chem. Soc.* **1995**, *117*, 1225.

7. (a) Blaskó, A.; Browne, K. A.; He, G.-X.; Bruice, T. C. *J. Am. Chem. Soc.* **1993**, *115*, 7080; (b) Blaskó, A.; Browne, K. A.; Bruice, T. C. *J. Am. Chem. Soc.* **1994**, *116*, 3726.

8. Loontiens, F. G.; Regenfuss, P.; Zechel, A.; Dumortier, L.; Clegg, R. M. *Biochemistry* **1990**, *29*, 9029.

9. Browne, K. A.; He, G.-X., Bruice, T. C. *J. Am. Chem. Soc.* **1993**, *115*, 7072.

10. Coll, M.; Frederick, C. A.; Wang, A. H.-J; Rich, A. *Proc. Natl. Acad. Sci. U.S.A.* **1987**, *84*, 8385.

11. Blaskó, A.; Bruice, T. C. *Proc. Natl. Acad. Sci. U.S.A.* **1993**, *90*, 10018.

12. Wemmer, D. E. In *Carbohydrates and Nuclic Acids*; Berliner, L. J.; Rueben, J., Eds.; Plenum: New York, 1992; Vol. 10, p 195.

13. (a) Sanger, F.; Air, G. M.; Barrell, B. G.; Brown, N. L.; Coulson, A. R.; Fiddes, J. C.; Hutchison, C. A. III; Slocombe, P. M.; Smith, M. *Nature* **1977**, *265*, 687; (b) Sanger, F.; Coulson, A. R.; Friedmann, T.; Air, G. M.; Barrell, B. G.; Brown, N. L.; Fiddes, J. C.; Hutchison, C. A. III; Slocombe, P. M.; Smith, M. *J. Mol. Biol.* **1978**, *125*, 225.

14. Hansma, H. G.; Browne, K. A.; Bezanilla, M.; Bruice, T. C. *Biochemistry* **1994**, *33*, 8436.

15. Wu, H.-M.; Crothers, D. M. *Nature* **1984**, *308*, 509.

16. Hore, P. J. *J. Magn. Reson.* **1983**, *55*, 283

17. Sambrook, J.; Fritsch, E. F.; Maniatis, T. *Molecular Cloning, A Laboratory Manual, 2nd Edition*; Cold Spring Harbor: New York, 1989.

18. Turro, N. J. *Modern Molecular Photochemistry*; The Benjamin/Cummings: Menlo Park, 1978; pp 311–319.

19. Browne, K. A.; Blaskó. A.; Bruice, T. C. *Bioorg. Med. Chem.* **1995**, *6*, 631.

20 (a) CHARMm (Version 22 interface) and QUANTA (Version 4.0), **1994**, distributed by Biosym/Molecular Simulations, Inc., Burlington, Massachussetts; (b) Momany, F. A.; Rone, R. *J. Comp. Chem.* **1992**, *13*, 888.

(*Received in U.S.A.* 9 *October* 1995; *accepted* 15 *February* 1996)